Modelling Simul. Mater. Sci. Eng. **6** (1998) 493–506. Printed in the UK PII: S0965-0393(98)94335-2

Effects of alloying on the ductility of $MoSi_2$ single crystals from first-principles calculations

U V Waghmare†, Efthimios Kaxiras†, V V Bulatov‡ and M S Duesbery§

† Department of Physics, Harvard University, Cambridge, MA 02138, USA
‡ Department of Mechanical Engineering, MIT, Cambridge, MA 02139, USA
§ Fairfax Materials Research, Inc., Springfield, VA 22153, USA

Received 2 February 1998, accepted for publication 7 May 1998

Abstract. The effects of substitutional alloying on the ductility of $MoSi_2$ single crystals are studied, using first-principles total energy calculations. The results are expressed in terms of a disembrittlement parameter, based on fracture mechanics theory, which characterizes brittle versus ductile behaviour. Substitution of Mo by V, Nb, Tc and Re and substitution of Si by Mg, Al, Ge and P was considered. The effects of substitution of Mo by V or Nb, and substitution of Si by Mg or Al are found to be particularly beneficial to the enhancement of ductility. The examination of self-consistent electronic charge distributions elucidates the changes in bonding responsible for changes in ductility.

1. Introduction

The use of advanced materials requires tailoring their properties to specific technological demands. While certain properties of a material may show promise for important applications, other aspects of its behaviour may render its manufacturing or ease of application rather difficult. A case in point is $MoSi_2$. With its high-temperature ductility and exceptional resistance to corrosion and fatigue crack growth, $MoSi_2$, a compound which combines the toughness of a metal with the strength of a ceramic, is a promising candidate to replace nickel superalloys in the next generation of high-temperature gas turbines. Unfortunately, it undergoes a ductile–brittle transition (DBT) at 1200 °C, with the fracture toughness dropping to 2–3 MPa $m^{1/2}$. This brittleness at low temperature, meaning as it does that $MoSi_2$ must be formed by costly electro-discharge machining, places a severe limitation on potential technological applications.

To make possible the use of this promising material in technological applications, it is desirable to alter its properties in very specific ways. This can be attempted by changing the composition or structure of the material and studying experimentally the effects of these changes. Advances in the theory of bonding in solids, based on quantum mechanical density functional theory calculations, and the ability to study complex solids using modern computational resources, may provide an alternative to costly trial-and-error experimentation.

In the case of $MoSi_2$, the need is for an element or elements which can be introduced at microalloy levels ($< 5\%$) and which will perturb the brittle–ductile behaviour in favour of ductility without adversely affecting the advantageous physical properties of $MoSi_2$. The purpose of the work reported here is to provide a guide to experiment by predicting which alloying elements are likely to produce favourable changes in the relative probabilities of

0965-0393/98/040493+14$19.50

fracture and plasticity in $MoSi_2$. While the method of choice would normally be an atomistic calculation [1], bonding in $MoSi_2$ is known to have hybrid metallic and covalent character [2]. Treatment of the effects of alloying on such bonding requires accurate quantum mechanical treatment of the electrons, and generation of reliable interatomic potentials which are an essential prerequisite to atomistic methods is impractical. Instead, use is made in the present work of recent advances in the theory of dislocation nucleation [3] and mobility [4] which provide approximate links between these properties and specific characteristics of the generalized stacking fault energy surface [5]. The latter can be calculated accurately using first-principles quantum mechanical techniques. A similar approach has been used successfully by two of the present authors to investigate related issues silicon [6]. Even with these approximations, the numerical work is intensive. Calculations are therefore restricted to small supercells, with correspondingly large alloy content. Despite these limitations, it is considered that the procedures used provide valuable physical insight and represent a rational, cost-effective option for guidance of experiment when compared with the heuristic alternative.

The paper is organized as follows. Section 2 contains an overview of experimental results related to attempts to enhance the ductility of $MoSi_2$. In section 3.1 the background to the criteria used to assess ductile and brittle response is outlined. The density functional methods which were used to obtain the model parameters are described in section 3.2. Section 4 contains the results for monolithic $MoSi_2$. In section 5, we discuss the changes which occur after substitutional alloying for either Si or Mo. Finally, we will conclude in section 6 with an assessment of the results and their implications for future work.

2. Review of experiments

Several attempts to improve the low-temperature fracture toughness of $MoSi_2$ by forming composite materials have been made. The addition of ceramic particles or whiskers such as SiC [7] or ZrO_2 [8] inhibits fracture and increases the fracture toughness to a level achieved by incorporation of a ductile second phase. For example, Mo in $MoSi_2$ [9] increases the fracture toughness (up to $\sim$10 MPa $m^{1/2}$). This is believed to be due to the crack-slowing effects of large matrix–particle interfacial stresses. The addition of carbon [10] scavenges silica from the grain boundaries, changing the fracture mode from intergranular to transgranular and increasing fracture toughness to 12 MPa $m^{1/2}$. The addition of carbon-lubricated silicon carbide continuous fibres increases the fracture toughness [11] to 35 Mpa $m^{1/2}$ for cracks normal to the fibre length. Unfortunately, the toughness for cracks running parallel to the fibres is unaffected. This process is costly and not easily extended to three dimensions, making it an unsuitable candidate for practical use.

The effect of structural modification on the DBT in $MoSi_2$ has also been examined, but the conclusions are conflicting. The tetragonal $C11_b$ structure of $MoSi_2$ is an ABAB... stacking of identical 110 planes. The related hexagonal C40 structure, which has been reported to occur in $MoSi_2$ at high temperatures, is an ABCABC... stacking of the same (now {0001}) planes. The transformation between the two lattices is accomplished by motion of (in $C11_b$ notation) $a/4\langle 111\rangle$ partial dislocations on {110} planes. This led to an idea [12] that phase destabilization—i.e. decreased stacking fault energy—could activate slip of partial dislocations on {110} planes and thereby increase ductility. Single crystal tests were performed [13] on $MoSi_2$ ($C11_b$), and the related silicides Cr, Ta, $NbSi_2$ (C40), Ti_5Si_3 ($D8_8$), and Co, $(Co, Ni)Si_2$ (C1). All the C40 structures were found to be ductile at RT (Cr the least so). The C1 structures were also ductile, but were found to have low melting points (1300 °C). The $C11_b$ and $D8_8$ structures were brittle at low temperatures. However, the observation of $a/4\langle 111\rangle$ faults (and hence the existence of $a/4\langle 111\rangle$ partial dislocations) in $MoSi_2$ has been questioned; transmission electron microscopy (TEM) diffraction analysis [14] shows the faults to be $a/6\langle 001\rangle\{001\}$, corresponding to a missing plate of silicon. The question of disembrittlement by phase destabilization therefore remains open.

There has also been some work, similarly inconclusive, on the effect of chemical alloying. Chin *et al* [15] examined a wide range of ternary $MoSi_2$ alloys. They considered the substitution of Al, B and Ge for Si and Hf, Nb and Re for Mo. For substitution of Al at 20% and 50% of the Si sites, the compound structure was the hexagonal C40. B was found to be insoluble. For Ge at 10%, 20% and 50% of Si sites, the $C11_b$ structure was maintained. Hf was insoluble. For Nb at 50% Mo sites, the structure changed to C40. For Re at 10%, 20% and 50% of Mo sites, the $C11_b$ structure was retained. All ternaries were tested both at room temperature and at high temperature. No significant change in the DBT temperature was found for any of the alloys. The addition of 10% Al (which is sufficient to cause a transformation to the C40 structure) to $MoSi_2$ was found to decrease the ductility and fracture toughness [16]. However, the addition of small amounts of Al lowers the hardness of polycrystalline $MoSi_2$ [17] and both lowers the hardness and increases the fracture toughness of single crystal $MoSi_2$ [18]. A small amount of Cr (3%) has also been reported to improve ductility [19].

The onset of brittleness is usually due to an increased difficulty in dislocation nucleation or mobility relative to cleavage. That this may be true at the DBT in $MoSi_2$ is supported by experiment [20]; prestraining at 1300 °C (which introduces additional dislocations when the material is ductile) increases the ductility of polycrystalline $MoSi_2$ at 800 °C from zero to 5%, at 750 °C to 1.5%. Further confirmation comes from single crystal experiments [21], which show that orientations other than those close to [001] are ductile down to room temperature. For orientations close to [001], plastic deformation occurs on the $\{013\}\langle 331\rangle$ system; the flow stress on this slip system increases rapidly as the DBT temperature is approached from above, indicating a sharp decrease in dislocation mobility. The evidence, therefore, indicates that the onset of brittleness in $MoSi_2$ is due to the loss of plasticity on this slip system, leaving no means of accommodation for the component of deformation parallel to the [001] axis.

3. Methods

3.1. Criteria for ductility and brittleness

There is general agreement that the fundamental competition between brittleness and ductility takes place at the crack tip, at which the applied stress is magnified by the lenticular shape of the crack [22]. The competing processes which lead to brittle or ductile behaviour are the extension of the crack by creation of fresh surfaces (brittle response) or the generation of dislocations that exert a back stress which reduces or *shields* the stresses and blunts the crack tip (ductile response). In the former process, the energy required for an incremental advance in the crack front is

$$G = 2\gamma_s \tag{1}$$

where G is the energy release rate (the mechanical energy released per unit area swept by the crack front) and γ_s is the surface energy (the energy needed to create a unit area of fresh surface). For the latter process, three principal theories offer different explanations. The Rice model [3] considers the governing mechanism to be the nucleation of dislocations at the crack tip. Hirsch and Roberts [23] assume that the critical step is not the nucleation of dislocations, but their motion away from the crack tip. The third point of view is that of Khantha *et al* [24], who argue that the shielding dislocations are nucleated in the part of the bulk material which lies within the stress field of the crack tip, by a Kosterlitz–Thouless-type mechanism [25].

In each of these theories the critical parameter is a property of the generalized stacking fault (γ-) surface [5], defined as follows: consider a crystal cut into two halves parallel to the (hkl) plane and suppose that one half is displaced relative to the other by the vector $\boldsymbol{f}$. As this vector is varied to span a unit repeat area in the plane of the cut, the energy $\gamma(\boldsymbol{f})$ of the crystal changes and traces out the γ-surface, which is normally expressed as an energy per unit area. Rice pointed out that in order to nucleate a dislocation with Burgers vector $\boldsymbol{b}$, it is necessary to follow a path on the γ-surface over which the displacement vector $\boldsymbol{f}$ changes continuously from 0 to $\boldsymbol{b}$. At some point along this path the energy reaches a maximum, which Rice calls the unstable stacking fault energy, γ_{us}. This quantity is critical to both the Rice and Khantha–Vitek models of the DBT. Within the Rice model, the criterion for dislocation emission is

$$G = \alpha\gamma_{\mathrm{us}} \tag{2}$$

where α is a factor of order unity which depends on the geometry of the crack.

In each of the models and in the Hirsch–Roberts model in particular, it is essential to ductility that the nucleated dislocations be able to move away from the crack tip easily. Without this freedom of motion it would not be possible to generate a density of dislocations sufficient to shield the crack tip stresses. Dislocation mobility can be estimated without recourse to atomistic methods using the approximate Peierls–Nabarro model [26], which for narrow dislocations can be formulated in terms of the maximum gradient of the γ-surface along the path to γ_{us} [4].

To summarize, the conditions for both brittle fracture and the nucleation and motion of dislocations can be expressed in terms of γ-surface features. If we adopt the view that dislocation nucleation is a necessary precursor of dislocation motion, the conditions become particularly simple, depending only on the two energies γ_{s} and γ_{us}. Brittleness will occur if the condition (1) is satisfied before (2); if the converse is true, the material will be ductile. We define a ‘disembrittlement parameter’

$$D = \frac{\gamma_{\mathrm{s}}}{\gamma_{\mathrm{us}}}.$$

The value of D that corresponds to the DBT is not known with any precision, but has been estimated [3] between 1 and 10. For present purposes, that is, to assess whether an alloying element enhances or degrades the ductility of $MoSi_2$, it is sufficient to determine whether the dopant increases or decreases the value of D relative to its value in the ideal crystal.

3.2. First-principles methods

Our first-principles total energy method is based on the local density approximation [27] (LDA) to density functional theory [28] (DFT). We use a pseudopotential approximation to represent the ion–electron interaction and a plane wave basis to represent the electronic wavefunctions and charge density. This type of calculation for simple systems such as Si and Al has proven very reliable in the study of structural properties of bulk and surfaces. We use optimized pseudopotentials [29] for transition metals (Mo, V, Nb, Tc and Re) with semicore s and p levels treated as valence states. Our calculations for the lattice constant and bulk modulus of the bulk elemental crystals and $MoSi_2$ resulted in excellent agreement with experiment.

An energy cutoff up to 60 Ryd has been used in these calculations to ensure convergence of energy differences within 1 mRyd atom. A Fermi–Dirac broadening scheme with $k_B T = 0.04$ eV is used to represent the Fermi surface discontinuity and 343 k-points are used to sample the Brillouin zone of a single unit cell of $MoSi_2$. At an energy cutoff of 60 Ryd, a calculation with three formula units of $MoSi_2$ per cell involves finding the lowest 40 eigenstates of a matrix of size 5000 for any given k-point. For efficient calculations on metallic systems involving large unit cells and surfaces, we use a preconditioned conjugate gradient algorithm [30] to iteratively diagonalize the Kohn–Sham Hamiltonian and the Kerker charge density mixing scheme [31] in the self-consistent procedure to avoid sloshing of charge between the vacuum and the slab region. This special charge density mixing scheme mixes small wavevector components of the charge density gradually and thereby damps oscillations during the self-consistency cycle.

Surface energies γ_s are obtained from the difference between the total energy E_{tot} of a crystal cleaved across a given plane and of the bulk. Our first-principles calculations use periodic boundary conditions, hence in practice we consider a periodic supercell and calculate its total energy as a function of d, the distance between two atomic layers separated by the desired cleavage plane in the supercell. These energies are fit to the universal binding energy function [32]

$$e(d) = \frac{E_{tot}(d)}{A} = e_\infty - 2\gamma_s(1 + x)e^{-x} \tag{3}$$

where $x = (d - d_{bulk})/\lambda$, e_∞ is energy per unit area (A) of the cleaved crystal, d_{bulk} is the interplanar separation of the bulk crystal and λ a length scale parameter. The unstable stacking fault energy is obtained from the total energy of a supercell containing the cut plane and with atoms on the two sides of the plane displaced in the direction of the fault vector with respect to each other.

4. Model analysis and results: $MoSi_2$

$MoSi_2$ crystallizes in a body-centred tetragonal structure as shown in figure 1(a), formed by the alternate stacking of single Mo and double Si (001) layers. Both Mo and Si atoms are highly coordinated, with 10 nearest neighbours; as expected with this coordination level, $MoSi_2$ is metallic. It has been found experimentally that many slip systems in $MoSi_2$ remain active at low temperatures [21]. Brittle failure in single crystals occurs only when the stress axis is close to [001] and is caused by increasing difficulty in operation of the slip system $\{013\}\langle 331\rangle$, shown in figure 1(b). This slip system involves motion of dislocations with $\frac{1}{2}[331]$ Burgers vector on (013) planes. To assess ductility trends, we calculate γ_s for (001) cleavage planes and γ_{us} for the $\{013\}\langle 331\rangle$ slip system from first principles.

In $MoSi_2$, there are two types of (001) cleavage planes: one separating adjacent layers of Si atoms and another separating adjacent layers of Mo and Si atoms. We use a supercell consisting of six (001) atomic layers (conventional tetragonal unit cell with 2 $MoSi_2$ formula units) in the calculation of γ_s. In figure 2, we show total energies for the two (001) surfaces fitted to equation (3). Energies in the limit of infinite interplanar separation with respect to the minimum (bulk energy) give the surface energies. Our results show that binding between (001) Si planes ($\gamma_s = 2.74$ J m^{-2}) is weaker than that between (001) Mo and Si planes ($\gamma_s = 3.94$ J m^{-2}). Since the surface relevant to brittle failure is that with the smaller γ_s, we shall focus on the energetics of cleavage between (001) silicon planes in the alloy calculations below.

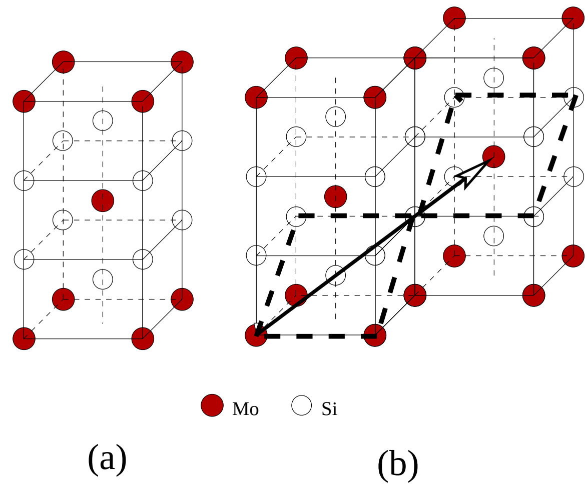

Figure 1. Crystal structure of $MoSi_2$: (a) unit cell for the body-centred $C11_b$ crystal; full circles represent Mo atoms and open circles represent Si atoms. (b) (013) plane and the Burgers vector for the slip system (013)[331].

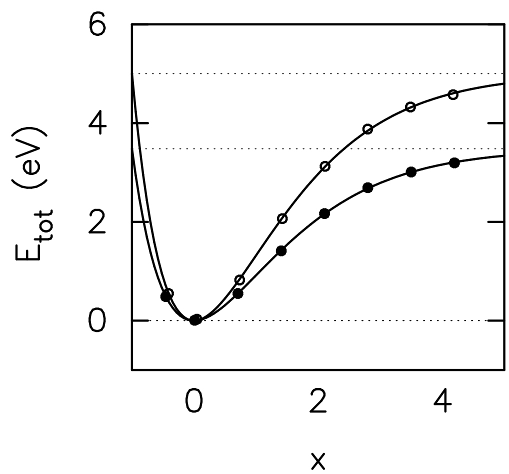

Figure 2. First-principles energies (points) fit to the universal equation of state (full curves), for pure Mo–Si (open circles) and Si–Si (full circles) cleavage planes of $MoSi_2$. As defined in text, x is the distance between the two adjacent atomic layers in the units of the length scale parameter λ.

To obtain a microscopic picture of bonding and better understanding of the above results, we examine the electronic charge densities in various planes of $MoSi_2$. In figure 3(a), we show plots of the electronic charge density in a (110) plane, which contains all the bonds that are broken in a (001) cleavage. Due to the contribution from core 4s and 4p electrons, there are large densities at Mo sites, indicated by red colour (top of the scale). Clearly, there is directional bonding between nearest-neighbour Mo and Si atoms appearing as triangular yellow regions, indicating covalent character. In contrast, there is no significant bonding between Si–Si and Mo–Mo atoms. This naturally results in lower cleavage energies for (001) planes that separate Si-planes. We also display charge densities in (001) planes in

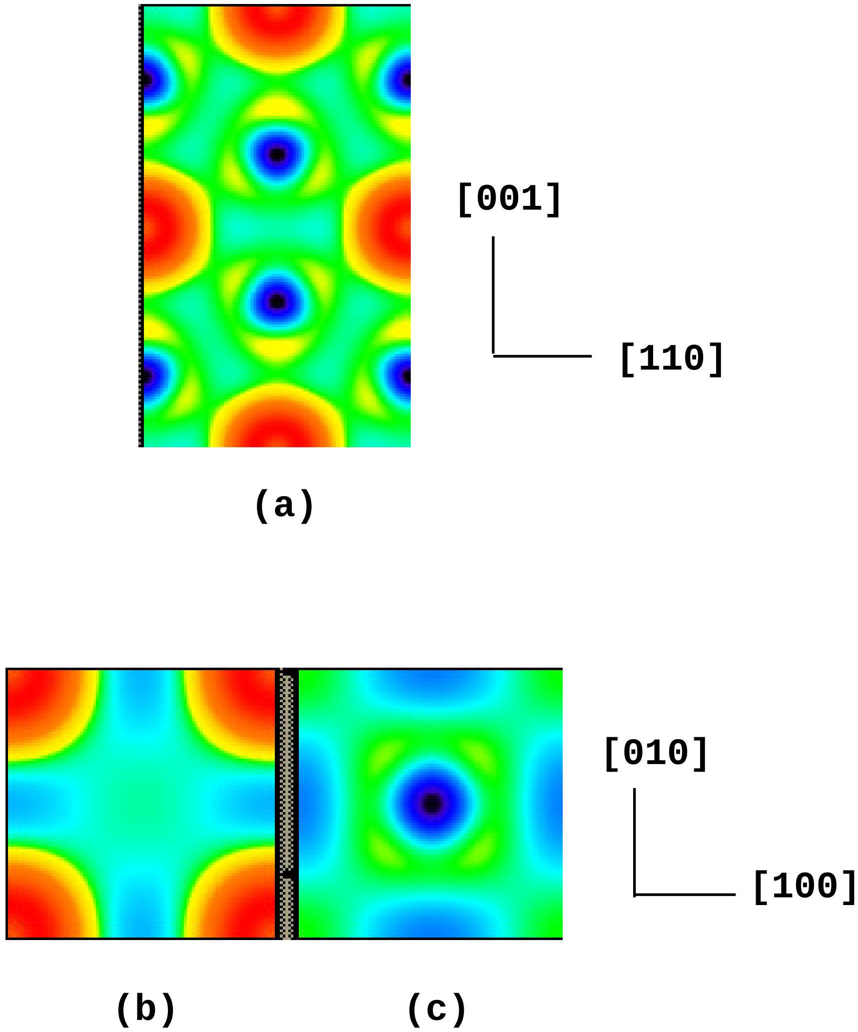

Figure 3. Electronic charge densities of $MoSi_2$ in (a) the (110) plane, (b) the (001) plane of Mo atoms and (c) the (001) plane of Si atoms. Red colour corresponds to large and purple to small charge densities. Mo atoms are at the centre of circular red regions in (a) and (b), and Si atoms are at the centre of circular black regions in (a) and (c).

figures 3(b) and (c). For both Mo and Si (001) layers, the charge densities are close to being isotropic. In addition, the small variation in charge density of Si layers indicates metallic character.

The atomic arrangement in the (013) plane is shown in figure 4(a) with the two smallest Burgers vectors, $b_0 = \frac{1}{2}[131]$ and $b = \frac{1}{2}[331]$. This plane is treated as a basal plane of a supercell used in the calculation of the stacking fault energy surface. We considered supercells with two and three (013) atomic planes to check convergence of the results with respect to supercell size, for a few points on the γ-surface. All the results for the γ-surface presented here have been obtained with calculations for a three-layer supercell, shown in figure 4(b). In figure 5 we show cross sectional branches of the generalized stacking fault energy surface along the two Burgers vectors. We find $\gamma_{us} = 4.33$ J m^{-2} for

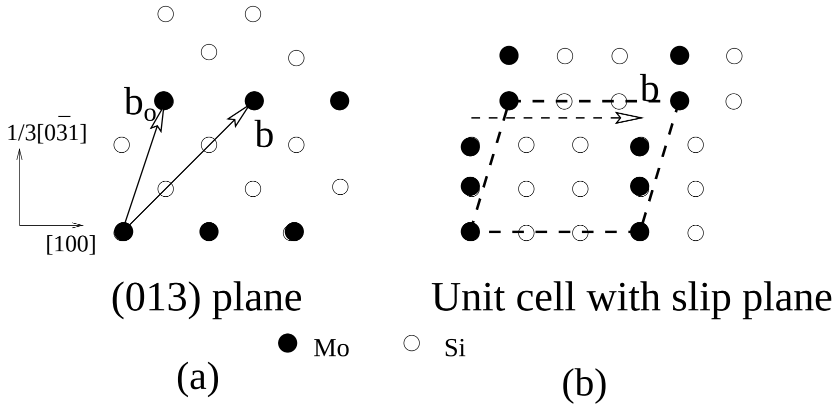

Figure 4. (a) Atomic arrangement in the (013) plane and the two smallest burgers vectors. (b) Schematic geometry of the three-layer supercell (side view) used in the calculation of slip energies. The dashed arrow indicates displacement of the upper half relative to the lower half of the crystal along a Burgers vector. The thick dashed line indicates the boundary of the supercell corresponding to a finite relative slip of the two halves.

the slip system {013}⟨131⟩ and $\gamma_{us} = 2.99$ J m^{-2} for the slip system {013}⟨331⟩, showing that the nucleation of dislocations on the latter system is energetically favoured, despite the longer Burgers vector. The intermediate energy minima along these curves indicate possible stable stacking faults. Connection of these results to possible dislocation dissociation and anti-phase boundary faults in $MoSi_2$ is the subject of [33].

5. Effects of substitutional alloying

In the previous section, we determined the properties of the cleavage and slip systems relevant to the ductile–brittle transition in $MoSi_2$ using a combination of first-principles calculations and experimental information for the relevant cleavage plane and slip system. To study the effects of substitutional alloying on ductility, we calculate the surface and unstable stacking fault energies for these planes using ordered supercells with a few of the Si or Mo atoms substituted with alloying elements. While the effects of disorder in such alloys are ignored, the goal here is to examine the effects of a specific alloying element on the bonding in $MoSi_2$ through changes it induces to the disembrittlement parameter D.

First we study the effects of Al substitution for Si in detail. We replaced a single (001) plane of silicon atoms with aluminium and calculated surface energies for various (001) planes, shown schematically in figure 6. We find that γ_s for most of the (001) cleavage planes reduces with Al substitution. Effects on the γ_s for cleavage at Si–Si planes are much stronger than those for cleavage at Mo–Si planes. These effects are strongly localized, decaying rapidly with distance normal to the plane of Al substitution. To obtain a microscopic picture, we examine the electronic charge densities for Al-substituted (50% and 100% planar substitution) $MoSi_2$, shown in figure 7. This corresponds to 16% and 33% substitution by volume or 4.4% and 8.9% substitution by weight, respectively. Comparison to the ideal $MoSi_2$ crystal, also shown in figure 7(c) reveals that the changes in charge densities are localized near the plane of Al substitution. These effects become stronger with concentration of planar substitution. The bonding of Si atoms in the plane of substitution with neighbouring atoms gets substantially reduced, hence the value of γ_s for cleavage near these planes is more severely affected than for other planes.

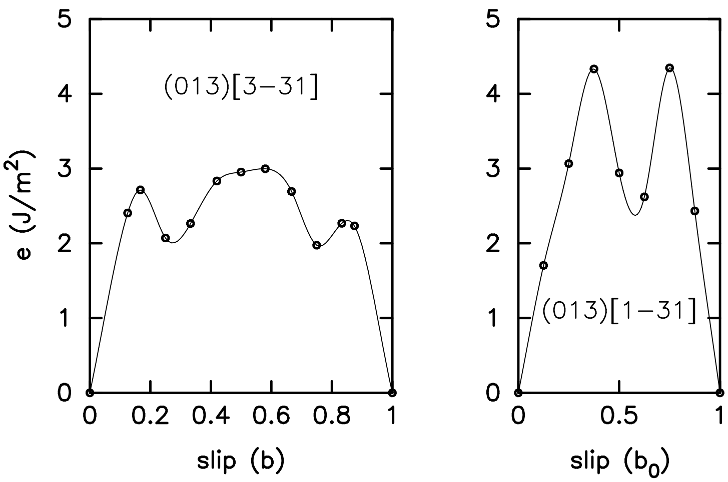

Figure 5. Energy per unit area of slips on the (013) plane of $MoSi_2$ in ⟨131⟩ and ⟨331⟩ directions, corresponding to the two vectors shown in figure 4(a). The curves through the points are cubic spline fits.

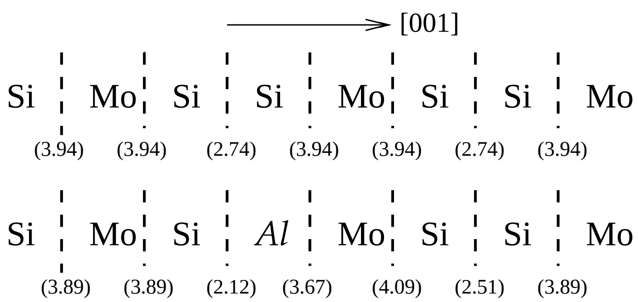

Figure 6. A schematic representation of the $MoSi_2$ crystal. Each element symbol represents an entire (001) plane of atoms of this type, while the dashed lines represent cleavage planes. The numbers in parentheses are the calculated surface energies (γ_s) for cleavage on those planes. The representation and numbers at the bottom are for a crystal with an entire Si plane near the middle of the slab substituted by Al.

The unstable stacking fault energies for Al-substituted $MoSi_2$ are obtained by replacing half or all of the Si atoms in the operative (013) slip plane. With 100% planar substitution (33% by volume) of aluminum for silicon, γ_{us} is reduced by 29%. These calculations did not include atomic relaxation. To estimate the effects of relaxation, we calculated the energies of a configuration corresponding to the highest energy barrier, and find that while the atomic relaxation reduces γ_{us} by 12 to 20%, the percentage reduction in γ_{us} (relative to its value in the ideal crystal) due to Al substitution remains essentially unchanged. We have also studied how the effects of Al-substitution on γ_s and γ_{us} change with its concentration. We calculated these quantities for 0 (pure $MoSi_2$), 50% and 100% planar concentrations of Al, and the results are shown in figure 8. The reduction in γ_{us} (shown in figure 8 as full circles) varies nearly linearly with Al concentration. The percentage reduction in γ_{us} is larger than that in γ_s for all the concentrations considered and particularly for small concentrations and hence the disembrittlement parameter D is enhanced as shown in the figure 8.

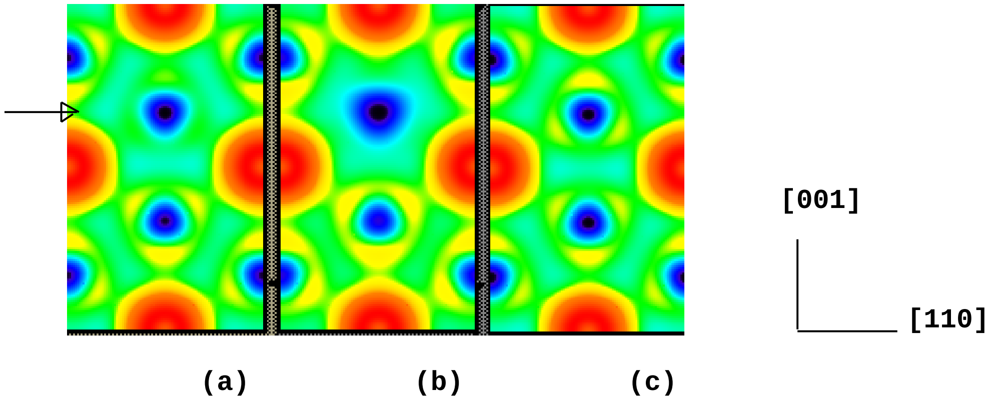

Figure 7. Electronic charge densities on the (110) plane of Al-substituted $MoSi_2$ with (a) 50% and (b) 100% planar substitution (Al atoms are substituted in the third atomic layer from top indicated by an arrow). For comparison, we display the charge density of monolithic $MoSi_2$ in (c).

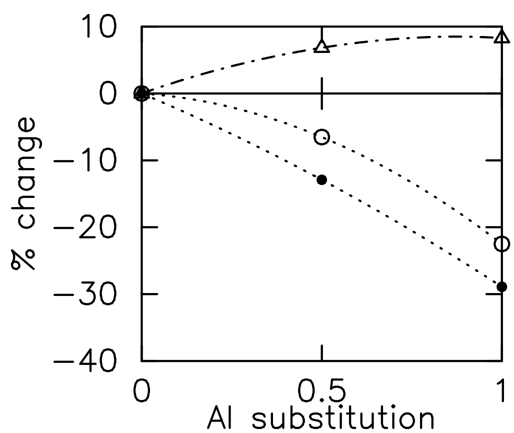

Figure 8. Percentage reduction in γ_s (open circles), γ_{us} (closed circles) and D (open triangles) as a function of planar concentration of Al substitution. The curves connecting these points are guides to the eye.

We conducted a more limited investigation into the effects of substitution of Mg, Ge and P for silicon. The results for γ_s and γ_{us} with full planar substitution are summarized in table 1. It is found that both γ_s and γ_{us} decrease for substitution by Mg and P. For Ge, γ_s decreases but γ_{us} increases slightly. Overall, the disembrittlement parameter D decreases with the number of valence electrons in the substituted element, indicating that alloying with acceptor elements should be better for the enhancement of ductility than alloying with isoelectronic or donor elements. Additional results (figure 9) for γ_{us} for substitution with these elements at 50% substitution reveal that, in general, γ_{us} varies to a good approximation linearly with concentration.

Finally, we explored the effects of substituting V, Nb, Tc and Re for Mo. The results for γ_s and γ_{us} are presented in table 2. As we have shown above, brittle failure breaks Si–Si bonds; therefore, substitution for Mo has little effect on γ_s. On the other hand, strong Mo–Si bonds are broken during dislocation nucleation, and hence any substitution for Mo

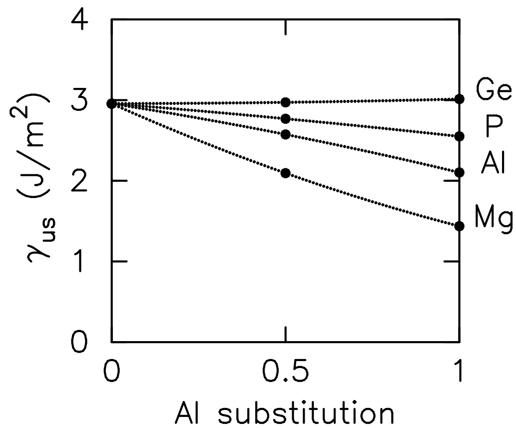

Figure 9. γ_{us} as a function of planar concentration of Mg, Al, Ge and P substitution for Si. The lines connecting these points are guides to the eye.

Table 1. Effects on γ_s and γ_{us} of full planar substitution of Si by Mg, Al, Ge and P. D is the disembrittlement parameter and D_0 its value for the ideal crystal ($D_0 = 0.92$).

Element	γ_s (J m^{-2})	γ_{us} (J m^{-2})	$(D - D_0)/D_0$
Si	2.74	2.99	0.00
Mg	1.61	1.45	0.21
Al	2.12	2.13	0.08
Ge	2.32	3.05	−0.17
P	1.78	2.58	−0.26

which weakens these bonds should and does lead to a reduction in γ_{us} comparable to that found in the substitution for Si. The disembrittlement parameter D increases with V, Nb and Tc substitutions, although, as for Si substitution, the effect is weaker for the alloying element with a higher valence charge. D decreases slightly with substitution of Re for Mo. The effects of V and Nb substitution on D are very similar, because of their same valence.

In figure 10, we display charge densities in (110) planes for the cases of 50% V and Tc substitution and compare them to the ideal $MoSi_2$ crystal charge density. In contrast with the substitutions for Si, the effects on charge density seem more extended here. The covalent nature of Mo–Si bonds persists, but is somewhat weaker. This is consistent with the small changes in γ_s we find with these substitutions. The effect of V substitution for Mo on the bonds with nearest-neighbour Si atoms is found to be stronger than that of Tc substitution for Mo.

6. Discussion and conclusions

The interpretation of macroscopic mechanical properties such as ductility and brittleness in terms of fundamental cohesive properties is a complex and difficult task. The present work uses a highly simplified treatment, which borrows heavily from fracture mechanics and dislocation theory, to make the connection between the macroscopic properties and first-principles quantum mechanical calculations to obtain reliable values for the crucial

Table 2. Effects on γ_s and γ_{us} of full planar substitution for Mo with V, Nb and Tc.

Element	γ_s (J m^{-2})	γ_{us} (J m^{-2})	$(D - D_0)/D_0$
Mo	2.74	2.99	0.00
V	2.49	2.30	0.18
Nb	2.60	2.42	0.18
Tc	2.35	2.34	0.10
Re	2.25	2.55	−0.04

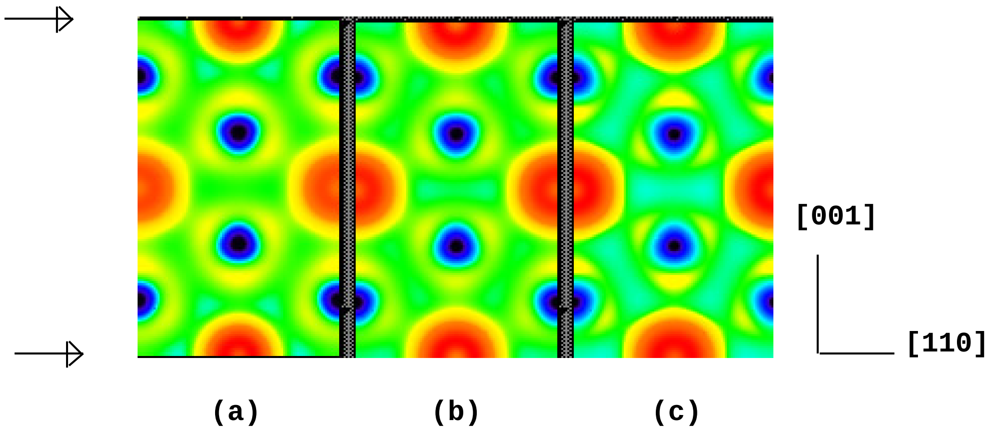

Figure 10. Electronic charge densities in the (110) plane of (a) V-substituted and (b) Tc-substituted $MoSi_2$ (V and Tc atoms are substituted for Mo atoms in the top and the bottom layers indicated by arrows). For comparison, we display the charge density of monolithic $MoSi_2$ in (c).

quantities that enter in the fracture mechanics analysis. There has been much work linking first-principles results to simpler macroscopic properties (for example, the elastic constants) for selected materials. To the authors' knowledge, the present work is the first of its kind in two respects: (i) it constitutes the first attempt to use first-principles, non-empirical techniques to provide a prescription for the design of materials with better ductility. (ii) It is the first of its kind to be motivated by a technological need and a philosophy of providing the most useful and relevant information, rather than by the cutting edge of scientific capability.

There are many approximations and simplifications which have been made in our approach. For example, the crystal structure of the alloys can differ from that of the matrix material, $MoSi_2$; we have assumed that the alloying element is soluble in $MoSi_2$ and the crystal structure remains the same. In a similar vein, sheer numerical complexity, even for this simple mode, has forced us to use small supercells. These correspond to large concentrations and ordered lattice sites for the alloying elements, even though our stated intention was to look at the *microalloy* regime. We make no attempt to justify these approximations, but rationalize them with the above-mentioned philosophy of providing the most useful and relevant information within the constraints of a real problem. Our results show trends for ductility which can be correlated with electronic structure, and which we expect to provide a cost-effective guide to experiment. We would especially like to emphasize that we were not aware of the recent experimental work [18, 34] confirming our calculated trends with aluminium substitution until after the present calculations were completed. This experimental confirmation is particularly gratifying in light of the drastic approximations employed.

In conclusion, using a simple model for ductile versus brittle response and input from first-principles calculations, we have studied the effects of substitutional alloying on the ductility of $MoSi_2$. This work is intended to provide a guide for experimental efforts to disembrittle $MoSi_2$ at low temperatures. Within the simplified treatment we predict that a quaternary compound which substitutes small concentrations of Mg or Al for Si and V or Nb for Mo will enhance ductility of $MoSi_2$ without significantly degrading its desirable physical properties.

Acknowledgments

This work was performed with support from the Office of Naval Research under SBIR contract No N00014-97-C-0104. Some of the calculations were performed using ACRES code developed under the CHSSI project. The authors wish to acknowledge useful discussions with Dr J J Petrovic (Los Alamos National Laboratory), Dr R J Hecht (Pratt & Whitney), N Bernstein, M Bazant, N A Modine, G Smith and E B Tadmor.

References

[1] Duesbery M S and Vitek V 1997 *Acta Mater.* at press
[2] Bhattacharya B K, Bylander D M and Kleinman L 1985 *Phys. Rev.* B **32** 7973
[3] Rice J R 1992 *Topics in Fracture and Fatigue* ed A S Argon (Springer)
Rice J R 1992 *J. Mech. Phys. Solids* **40** 239
Rice J R and Beltz G 1994 *J. Mech. Phys. Solids* **42** 333
[4] Joos B and Duesbery M S 1997 *Phys. Rev. Lett.* **78** 226
[5] Vitek V 1968 *Phil. Mag.* **18** 773
[6] Kaxiras E and Duesbery M S 1993 *Phys. Rev. Lett.* **70** 3752
[7] Bhattacharya A K and Petrovic J J 1992 *J. Am. Ceram. Soc.* **74** 1045
[8] Petrovic J J, Honnell R E, Mitchell T E, Wade T E and McClellan K J 1991 *Ceram. Eng. Sci. Proc.* **12** 1633
[9] Lu T C, Evans A G, Hecht R J and Mehrabian R 1991 *Acta Metall. Mater.* **39** 1853
[10] Maloy S, Heuer A H, Lewandowski J J and Petrovic J J 1991 *J. Am. Ceram. Soc.* **74** 2704
[11] Rawal S 1995 *Martin Marietta Astronautics, ONR Workshop on $MoSi_2$ (Hyannis, MA, June 1995)* unpublished work
[12] Umakoshi Y, Sakagami T, Yamane T and Hirano T 1989 *Phil. Mag. Lett.* **59** 159
Umakoshi Y, Sakagami T, Hirano T and Yamane T 1990 *Acta Metall.* **38** 909
[13] Umakoshi Y, Nakashima T, Nakano T and Yanagisawa E 1993 *MRS Symp. on High Temperature Silicides and Refractory Alloys (MRS Symp. Proc. 322)* ed C L Briant *et al* (Pittsburgh, PA: Materials Research Society) p 9
[14] Kad B K, Vecchio K S, Bewlay B P and Asaro R J 1993 *MRS Symp. on High Temperature Silicides and Refractory Alloys (MRS Symp. Proc. 322)* ed C L Briant *et al* (Pittsburgh, PA: Materials Research Society) p 49
[15] Chin S, Anton D L and Giamei A P 1993 *MRS Symp. on High Temperature Silicides and Refractory Alloys (MRS Symp. Proc. 322)* ed C L Briant *et al* (Pittsburgh, PA: Materials Research Society) p 423
[16] Inui H, Moriwaki M, Ito K and Yamaguchi M 1998 *Phil. Mag.* A **77** 375
[17] Costa e Silva A and Kaufman M J 1993 *Scr. Metall. Mater.* **29** 1141
[18] Peralta P, Chu F, Maloy S A, Santiago P, Petrovic J J and Mitchell T E 1997 *Scr. Mater.* **37** 1599
[19] Umakoshi Y, Hirano T, Sakagami T and Yamane T 1990 *TMS Symp. on High Temperature Aluminides and Intermetallics* ed S H Whang, C T Liu, D P Pope and J O Steigler (Warrendale, CA: TMS) p111
[20] Gibala R, Chang H and Czarnik C M 1993 *MRS Symposium on High Temperature Silicides and Refractory Alloys (MRS Symp. Proc. 322)* ed C L Briant *et al* (Pittsburgh, PA: Materials Research Society) p 49
[21] Ito K, Inui H, Shirai Y and Yamaguchi M 1995 *Phil. Mag.* A **72** 1075
[22] Inglis C E 1913 *Trans. Inst. Naval Arch.* **55** 219
[23] Hirsch P B and Roberts S G 1991 *Phil. Mag.* A **64** 55

[24] Khantha M, Pope D P and Vitek V 1994 *Phys. Rev. Lett.* **73** 684
[25] Kosterlitz J M and Thouless D J 1973 *J. Phys. C: Solid State Phys.* **6** 1181
[26] Peierls R 1940 *Proc. Phys. Soc.* B **52** 34
Nabarro F R N 1947 *Proc. Phys. Soc.* B **59** 256
[27] Ceperley D M and Alder B J 1980 *Phys. Rev. Lett.* **45** 566
Perdew J P and Zunger A 1981 *Phys. Rev.* B **23** 5048
[28] Hohenberg P and Kohn W 1964 *Phys. Rev.* B **136** 864
Kohn W and Sham L J 965 *Phys. Rev.* A **140** 1133
[29] Rappe A M, Rabe K M, Kaxiras E and Joannopoulos J D 1990 *Phys. Rev.* B **41** 1227
[30] Teter M P, Payne M C and Allan D C 1989 *Phys. Rev.* B **40** 12 255
[31] Kreese G and Furthmuller J 1996 *Comput. Mat. Sci.* **6** 15
[32] Rose J H, Smith J R, Guinea F and Ferrante J 1984 *Phys. Rev.* B **29** 2963
[33] Waghmare U V, Bulatov V, Kaxiras E and Duesbery M S 1998 *Phil. Mag.* A submitted
[34] Peralta P, Chu F, Maloy S A, Santiago P, Petrovic J J and Mitchell T E 1997 *Proc. AFOSR-sponsored International Conference on Computer-Aided Design of High-Temperature Materials, (30 July-2 August 1997, Santa Fe, New Mexico)*